AGU PUBLICATIONS

Geochemistry, Geophysics, Geosystems

RESEARCH ARTICLE
10.1002/2013GC005213

Key Points:
- Geochemical data provide strong evidence of active serpentinization
- Methanogenic Archaea suggest that methanogenesis is active in the area
- Serpentinization in a unique tropical environment

Supporting Information:
- Auxiliary Table A1-A6
- Auxiliary Figures 1-2
- ReadMe

Correspondence to:
E. Gazel,
egazel@vt.edu

Citation:
Sánchez-Murillo, R., E. Gazel, E. Schwarzenbach, M. Crespo-Medina, M. O. Schrenk, J. Boll, and B. C. Gill (2014), Geochemical evidence for active tropical serpentinization in the Santa Elena Ophiolite, Costa Rica: An analog of a humid early Earth?, *Geochem. Geophys. Geosyst.*, *15*, doi:10.1002/2013GC005213.

Received 23 DEC 2013
Accepted 12 APR 2014
Accepted article online 17 APR 2014

Geochemical evidence for active tropical serpentinization in the Santa Elena Ophiolite, Costa Rica: An analog of a humid early Earth?

Ricardo Sánchez-Murillo[1], Esteban Gazel[2], Esther M. Schwarzenbach[2], Melitza Crespo-Medina[3], Matthew O. Schrenk[3], Jan Boll[1], and Ben C. Gill[2]

[1]Waters of the West—Water Resources Program, University of Idaho, Moscow, Idaho, USA, [2]Department of Geosciences, Virginia Tech, Blacksburg, Virginia, USA, [3]Department of Geological Sciences and Department of Microbiology and Molecular Genetics, Michigan State University, East Lansing, Michigan, USA

Abstract Serpentinization is a planetary process that has important consequences on geochemical cycles, supporting microbial activity through the formation of H_2 and CH_4 and having the potential to sequester atmospheric CO_2. We present geochemical evidence of active serpentinization in the Santa Elena Ophiolite, Costa Rica which is sustained by peridotites with a degree of serpentinization less than 50% with no evidence of an internal heat source. Average spring water temperatures are 29.1°C. Two hyperalkaline spring systems were discovered, with a spring fluid pH up to 11.18. The fluids are characterized by low Mg (1.0–5.9 mg/L) and K (1.0–5.5 mg/L) and relative high Ca (29–167 mg/L), Na (16–27 mg/L), Cl (26–29 mg/L), hydroxide (41–63 mg/L), and carbonate (31–49 mg/L). Active CH_4 (24.3% v/v) vents coupled with carbonate deposits ($\delta^{13}C_{CO2} = -27$ to $-14‰$; $\delta^{18}O_{CO2} = -17$ to $-6‰$) also provide evidence for active serpentinization and carbonation. Isotope ratios of the alkaline fluids ($\delta^{18}O = -7.9‰$, $\delta^{2}H = -51.4‰$) and groundwater ($\delta^{18}O = -7.6‰$; $\delta^{2}H = -48.0‰$) suggests that, during base flow recession, springs are fed by groundwater circulation. Methanogenic Archaea, which comprises a relatively high percentage of the 16S rRNA gene tag sequences, suggests that biological methanogenesis may play a significant role in the system. Santa Elena's extreme varying weather results in a scenario that could be of significant importance for (a) improving the knowledge of conditions on a humid early Earth or Mars that had periodic changes in water supply, (b) revealing new insights on serpentinizing solute transport, and (c) modeling hydrogeochemical responses as a function of recharge.

1. Introduction

1.1. Serpentinization

Serpentinization—the reaction of ultramafic rocks with fluids to form serpentine—is a planetary process (i.e., Earth-like planets, moons, and undifferentiated bodies such as chondritic asteroids) that results in the formation of H_2 through oxidation of Fe^{2+} in the primary minerals and has been described in several systems both in seawater exposed mantle rocks along slow-spreading mid-ocean ridges and in ultramafic rocks emplaced on the continents [*Frost*, 1985; *Allen and Seyfried*, 2003; *Bach et al*., 2006; *Frost and Beard*, 2007; *Alt et al*., 2007, 2013; *Schwarzenbach et al*., 2013a].

The presence of H_2 and CH_4, the latter formed through abiotic reduction of CO_2 [*Proskurowski et al*., 2008; *Lang et al*., 2012], are major energy sources for microbial activity and have been shown to support prolific microbial communities in peridotite-hosted hydrothermal systems [*Kelley et al*., 2005; *Brazelton et al*., 2006, 2012; *Suzuki et al*., 2013; *Brazelton et al*., 2013]. Additionally, serpentinization of ultramafic rocks generally produces hyperalkaline fluids (pH > 10) with high Ca^{2+}, low Mg^{2+}, and low total carbon concentrations that also plays an important role in the abiogenic cycling of carbon [*Barnes et al*., 1967; *Neal and Stanger*, 1983; *Kelley et al*., 2001; *Schwarzenbach et al*., 2013a, 2013b; *Schrenk et al*., 2013].

Sections of mantle rocks exposed on the surface of our planet under subaerial conditions (named here *continental serpentinization*) provide natural laboratories to study present-day serpentinization [*Blank et al*., 2009; *Szponar et al*., 2012; *Schwarzenbach et al*., 2013b; *Chavagnac et al*., 2013; *Morill et al*., 2013; *Etiope et al*., 2013; *Pirard et al*., 2013] and potential geologic CO_2 sequestration [*Matter et al*., 2007; *Kelemen and Matter*, 2008; *Kelemen et al*., 2011; *Paukert et al*., 2012]. These laboratories serve as an analog to other terrestrial

planets and moons that have an ultramafic and mafic crust and contain liquid water and thus can give new insights into the occurrence of "habitable environments in the universe." Recent mapping efforts of Mars' surface have reported the dominance of mafic to ultramafic rocks [*Hoefen et al*., 2003; *Christensen et al*., 2005]. Ongoing initiatives on mid-ocean ridges and in ophiolites have already provided insight into the importance of this process for the life on our planet [*Schrenk et al*., 2004; *Brazelton et al*., 2006, 2010, 2013; *Schwarzenbach et al*., 2013a]. However, the factors (e.g., H_2, CH_4 fluxes, water input, pH, temperature gradients, and nutrient availability) that control the occurrence of microbial communities in these systems are still unknown. The presence of H_2 and CH_4 in the fluid controls the occurrence of biological activity, and methane and sulfur metabolizing microorganisms were found at the Lost City hydrothermal field, a peridotite-hosted hydrothermal system along the Mid-Atlantic Ridge [*Schrenk et al*., 2004; *Kelley et al*., 2005; *Brazelton et al*., 2006]. These systems are thought to be similar to those found in early Earth, leading to an increased interest in studying the ability of such environments to not only host the most primitive life-forms on Earth, but also to have served as a birth place of life [*Russell et al*., 1989, 1994; *Früh-Green et al*., 2004; *Holm et al*., 2006; *Schulte et al*., 2006; *Martin and Russell*, 2007]. Given their composition, other planets, planetesimals, or moons (such as Mars or Europa) hold the potential to host similar ecosystems [*Russell et al*., 1989; *Hand et al*., 2007; *Russell and Kanik*, 2010]. Presently, mantle-derived ultramafic rocks are ubiquitously exposed on the seafloor, in the forearc regions of some intraoceanic arcs and on continents by tectonic processes [*Cannat*, 1993; *Kelley et al*., 2001; *Cannat et al*., 2013]. However, ultramafic volcanic rocks were significantly more abundant on Earth's surface during the Archean [*Myers and Crowley*, 2000; *Nisbet and Sleep*, 2001].

On land, interaction of meteoric water with peridotites results in Mg-HCO_3 waters, which in the absence of a CO_2 source, progressively evolve to hyperalkaline Ca^{2+}-OH waters [*Bruni et al*., 2002; *Boschetti and Toscani*, 2008; *Marques et al*., 2008]. Despite presumably low reaction temperatures in the basement (50–100°C, as no heat source has been observed in any of the continental serpentinization sites), high methane and/or hydrogen concentrations were measured in the Voltri Massif, Italy [*Cipolli et al*., 2004], the Zambales Ophiolite, Philippines [*Abrajano et al*., 1988, 1990], in the Newfoundland Ophiolite, Canada [*Szponar et al*., 2012], in the Samail Ophiolite, Oman [*Neal and Stanger*, 1983], and in the Othrys Ophiolite, Greece [*Etiope et al*., 2013]. The availability of hydrogen—and thus indirectly the availability of methane—as an energy source for microorganisms may strongly be regulated by water-rock ratios (i.e., fluid fluxes) that influence the rate of serpentinization. Additionally, the availability of inorganic carbon in the fluids controls the amount abiogenic of methane formed. *Shervais et al*. [2005] suggested that the production of hydrogen may, to some degree, be self-sustaining due to the increase in volume and potential mechanical fracturing, consequently, exposing new unreacted mineral surface area to meteoric water and organisms. Despite the aforementioned models, the role—and importance—of new meteoric water and its subsurface transit time in continental serpentinization systems remains unclear both in temperate and tropical environments.

Interaction of the alkaline spring waters with atmospheric CO_2 results in the formation of carbonate deposits. Where Mg-HCO_3 waters discharge, magnesite is formed as the water gets oversaturated with respect to magnesite, while interaction of the Ca-OH fluids with atmospheric CO_2 results in the formation of calcite. Such calcite deposits usually precipitate at the exit sites of the alkaline spring waters, where they form carbonate crusts or travertines on the basement rock as abundantly observed in association with mantle rocks [e.g., *Neil and Stanger*, 1983; *Clark and Fontes*, 1990; *Kelemen and Matter*, 2008; *Chavagnac et al*., 2013; *Schwarzenbach et al*., 2013b]. Such carbonate deposits are typical features that indicate that the serpentinization process is occurring in the subsurface. At the same time, concentrations of other species that can serve as nutrients for microbial activity (e.g., DIC, SO_4) evolve as well, e.g., due to the interaction with sulfur- or carbon-bearing minerals in the peridotite (e.g., sulfide minerals, sulfate carbonates formed during seafloor serpentinization). Thus, the chemical evolution of the fluids is related to the subsurface serpentinization reactions that are controlled by the chemical composition of the primary peridotite, water input from the surface, or potential interlayered sediments when present. Methane in these systems may be derived from abiotic reduction of CO_2, in situ microbial activity, or have a primary mantle origin. Therefore, the amount of H_2 that is generated is likely controlled by the primary mineralogy (i.e., the amount of unaltered peridotite available) and the rate of serpentinization, which in turn is primarily controlled by temperature and the water-to-rock ratio.

1.2. Climate and Hydrogeological Uniqueness of the Santa Elena Ophiolite

The main objective of this study is to present geochemical evidence of a new tropical active serpentinization end-member discovered early in 2013 within the Santa Elena Ophiolite, Costa Rica. Extreme varying

climate conditions between dry and wet seasons result in a unique hydrogeological scenario that could be of significant importance for (a) improving current knowledge of conditions on a humid early Earth or Mars that had periodic changes in water supply [*Barron et al*., 1989; *Craddock and Howard*, 2002; *Paige*, 2005; *Fairén*, 2010], (b) revealing new insights on serpentinization processes and the natural release of hyperalkaline fluids as base flow, and (c) modeling hydrogeochemical responses as a function of meteoric water recharge and base flow recession in present-day continental serpentinization environments.

Commonly, continental serpentinization and hyperalkaline spring studies have been conducted in temperate regions (e.g., Tablelands, Canada; Western Coastal Range, USA; Gruppo di Voltri, Italy; Othrys, Greece) and at subtropical sites (e.g., Samail, Oman). In these regions, precipitation is mostly composed of snow events, meteoric recharge occurs in a short time during spring runoff or in relatively slow snowmelt rates. Coastal temperate sites might experience intermittent rainfall at relatively low intensities. Furthermore, in arid and semiarid areas where precipitation events are scarce and isolated, infiltration is limited due to large evaporation losses. Contrary to the previous scenarios, in tropical environments precipitation amounts and rainfall intensities are usually greater and occur throughout several months, which facilitate infiltration, and thus, water-rock interaction, may be exacerbated.

To our knowledge, this study constitutes the first comprehensive characterization of active serpentinization in a tropical environment and poses a novel opportunity to study the interplay between the hydrology, serpentinization, and life.

2. Study Area

2.1. Santa Elena Ophiolite and Sampling Locations

Geotectonically, Costa Rica is situated at the triple junction of the Cocos, Caribbean, and Nazca plates. Along the Middle American Trench, the subduction of the Cocos Plate underneath the Caribbean Plate results in an active volcanic front [*Carr et al*., 2007; *Saginor et al*., 2013]. Along the Pacific side of Costa Rica, several oceanic complexes have been accreted onto the Caribbean Plate [*Hauff et al*., 2000; *Denyer and Gazel*, 2009; *Herzberg and Gazel*, 2009, and references therein]. The Santa Elena Ophiolite is the northernmost of these oceanic complexes and comprises an area of 250 km^2 of mafic and ultramafic lithologies [*Gazel et al*., 2006] located in the Santa Elena peninsula within the Area Conservación Guanacaste (ACG, i.e., Guanacaste Conservancy Area). The structure of the Santa Elena Peninsula includes an ultramafic complex at the hanging wall and an igneous-sedimentary complex at the footwall—the Santa Rosa Acretionary complex [*Baumgartner and Denyer*, 2006; *Denyer and Gazel*, 2009]. The ophiolite (Figure 1) contains variably serpentinized peridotites, dunites, and locally layered gabbros. Various generations of pegmatitic gabbros and diabase dikes cut the peridotites. Some of these dikes do not preserve chilled margins, implying that they intruded into the mantle host when it was hot and plastic. A secondary mineralogy in the mafic lithologies composed of albite + epidote + actinolite + chlorite, and variable serpentinization in the peridotites is evidence of ocean floor metasomatism [*Gazel et al*., 2006]. The Santa Elena Ophiolite was correlated with other peridotites outcrops along the Costa Rica-Nicaragua border interpreted as E-W suture zone emplaced between different tectonic blocks [*Tournon et al*., 1995]. The fact that the Santa Elena complex is covered by Campanian-age rudists reef limestones suggests that the exhumation was active during the Upper Cretaceous [*Gazel et al*., 2006; *Denyer and Gazel*, 2009], nevertheless details studies are required to reconstruct the exhumation and tectonic history of this complex.

The ACG was included in the UNESCO World Heritage List in 1999 due to its unique terrestrial (i.e., presence of an ophiolite and the most important tropical dry forest in Mesoamerica) and marine-coastal environments. We conducted two field sampling campaigns in the Santa Elena Ophiolite (January and March 2013) during which we sampled groundwater (12 private and municipal wells outside of the ACG, 30–70 m depth), surface waters (27 locations), freshwater springs (10 sites), hyperalkaline springs (2 systems), mineral precipitates (17 samples), gas emissions (1 site), and microbial communities (2 sites) (Figure 1 and supporting information Table S1). A subset of water samples were selected for comprehensive geochemical analyses as shown in supporting information Tables S2 and S3.

Two main hyperalkaline systems were sampled within Murciélago and Potrero Grande rivers which constitute the most significant perennial streams in the area (Figure 1). Potrero Grande River is characterized by a 10.3 km long floodplain and relatively steep tributaries (~33% slope). Active erosion processes resulted in

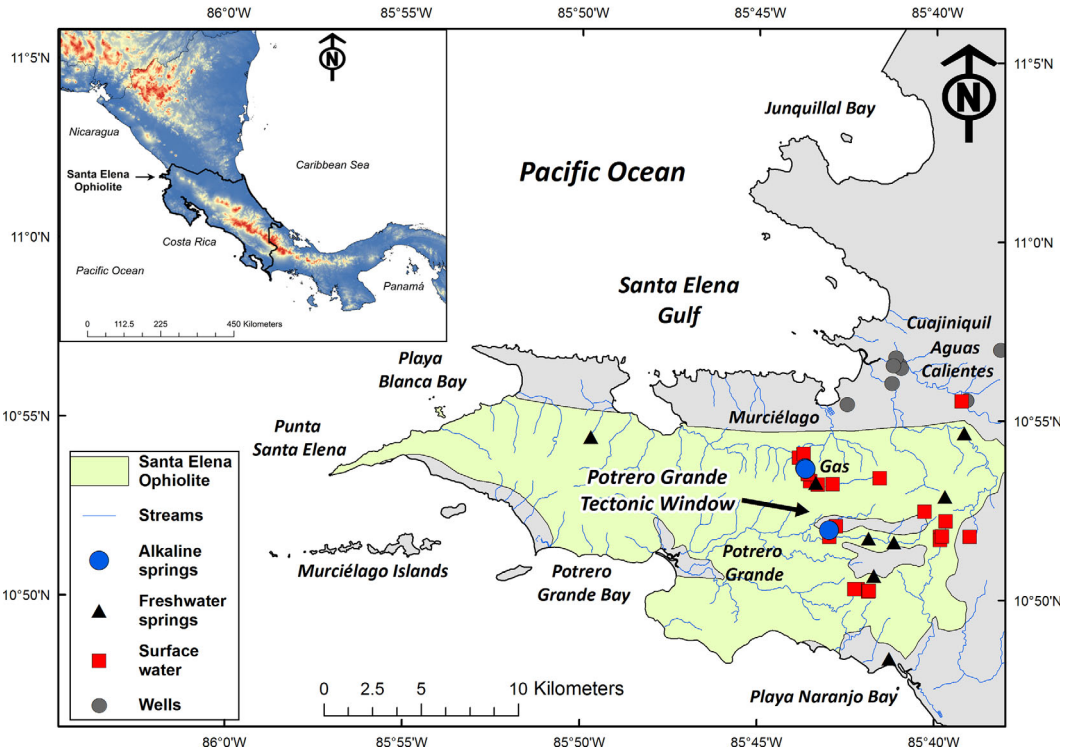

Figure 1. Map of the study area. Green highlighted area denotes Santa Elena Ophiolite, dominated by ultramafic mantle rocks based on *Gazel et al.* [2006]. Sample locations are color-coded: alkaline spring systems within Murciélago and Potrero Grande watersheds are identified by blue circles. Black triangles denote freshwater springs. Gray circles represent groundwater wells. Red squares stand for surface water sites. Blue lines are perennial and intermittent streams. Inset shows an overview of Central America.

the greater peridotite exposure among all watersheds in the Santa Elena peninsula. Vegetation (i.e., deciduous trees) is mostly located in riparian areas, whereas tropical dry forest grass is common on the upper part of the stream canyons. The hyperalkaline system within Potrero Grande is located in the headwaters about 121 m.a.s.l. Murciélago River is characterized by a relatively narrow valley and a greater presence of riparian vegetation. The hyperalkaline springs within Murciélago are located within the lower portion of the catchment (78 m.a.s.l.). Overall, field evidence suggests that hyperalkaline seepages are numerous and are active late in the base flow period of perennial streams. Hyperalkaline springs often form shallow pools characterized by moderate turbidity, thin white films of carbonates, and extensive yellow-brown carbonate deposits (Figures 2 and 3). Hyperalkaline fluids mixing with perennial receiving stream waters occurs at a low rate; therefore, dilution occurs rapidly. Sampling of hyperalkaline fluids was conducted directly at the spring outflow without the interference of stagnant or diluted stream waters.

2.2. Climate and Hydrological Singularities

The climate of Costa Rica is controlled by northeast trade winds, the shifts of the Intertropical Convergence Zone (ITCZ) and indirect influence of Caribbean cyclones [*Waylen et al.*, 1996]. These circulation processes produce two main seasons: the wet season (May–October) corresponds to the time when the ITCZ travels over Costa Rica, and precipitation is characterized by heavy convective rainstorms. The dry season (November–April) comprises the months when the ITCZ is to the south of Costa Rica [*Guswa et al.*, 2007]. The Santa Elena Peninsula receives on average 1464 mm/yr of rainfall (based on 10 years of historical records at the Santa Rosa climatological station, supporting information Figure S1). La Niña phenomena produce a considerable rainfall increase up to 3000 mm, while El Niño years are characterized by annual precipitation below 1200 mm and a dry period usually spans 5–7 months. Seasonal temperature variation is low; mean annual maximum and minimum ambient temperatures are 31°C and 23°C, respectively. During the dry period, maximum temperatures can reach up to 40°C. A summary of climate data for 2012 climatological water year conditions is presented in Figure 4 and additional years in supporting information Figure S1.

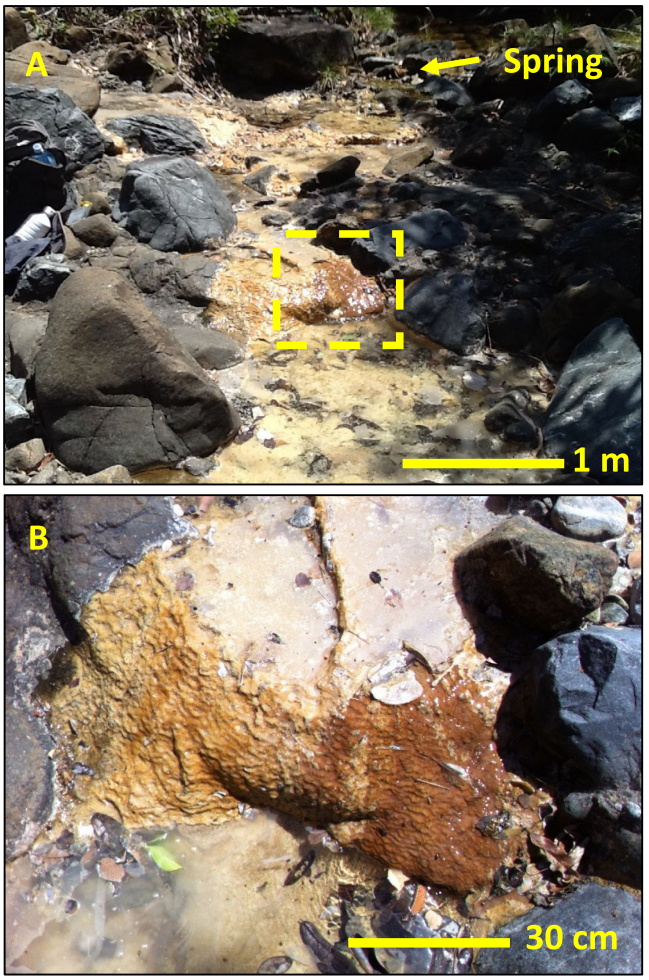

Figure 2. (a) Image of the hyperalkaline spring at Quebrada Danta site (within the Potrero Grande tectonic window) showing pool on the left stream bank with extensive yellow-brown precipitates. These precipitates form small travertine terraces. (b) Enlargement of yellow dash-square area. Note high water turbidity, organic matter, travertine deposits, and white supernatant crust are due to atmospheric CO_2 uptake.

The Northwestern Pacific region of Costa Rica has estimated regional groundwater recharge rates of less than 300 mm/yr [*Mulligan and Burke*, 2005]. Base flow recession starts in November and reaches its minimum in late April. Presumably, heavy convective storms produce flash runoff events. Most of the groundwater recharge in the peninsula occurs between July and October. Due to its UNESCO World Heritage status, the extent of hydrogeological research has been limited within ACG. Therefore, no hydraulic test and aquifer parameter information is available. Likewise, to our knowledge, long-term or current discharge data are not available for this area.

3. Sampling Methods and Analytical Techniques

3.1. Water Chemistry

A set of parameters (i.e., water temperature, pH, conductivity) were measured in situ with a portable probe (Model 99130, Hannah Instruments). This probe was calibrated twice a day using pH standard and conductivity solutions (HI 7000 Series, Hannah Instruments). Hyperalkaline fluids were sampled directly from seepage sources into sterile Nalgene HDPE bottles. A set of blank bottles containing ultrapure water was treated in the same manner as the samples. Samples were stored at 5°C, transported, and analyzed within 1 week of collection. Bottles for alkalinity analysis were filled completely (i.e., no head space) and covered with parafilm to avoid CO_2 exchange. Samples for determination of heavy and alkaline metals were acidified to a pH < 2 to prevent precipitation during storage. Samples were filtered through 0.45 μm glass fiber filters (Millipore) immediately after arrival in the laboratories. Samples for stable isotope analysis were collected in 30 mL glass E-C borosilicate vials with TFE-lined caps (Wheaton Science Products). Vials were filled without head space and covered with parafilm (Thermo Scientific) to avoid interaction with atmospheric moisture or fractionation.

Expanded alkalinity was analyzed by potentiometric titration [*Eaton et al.*, 1998, Standard Method 2320b]. The results obtained from the phenolphthalein and total alkalinities allowed the stoichiometric determination of bicarbonate, carbonate, and hydroxide, whose concentrations are reported as mg/L of $CaCO_3$ equivalent. Major and trace elements were measured by inductively coupled plasma optical emission spectrometry (Thermo Trace Jarrel-ash 51-*i*) [*Eaton et al.*, 1998, Standard Method 3120b]. Calibration was conducted using synthetic standards with a relative standard deviation (RSD) of 2% or better. Both expanded alkalinity major and trace elements analyses were conducted at the certified (INTE-ISO/IEC 17025:2005) Agrotec Analytical Laboratory (San José, Costa Rica). Ion concentrations were measured by ion chromatography (Model ICS-5000 Dual) with an electrical conductivity detector. Calibration was conducted using synthetic standards with a RSD of 3% or better. Stable isotope analysis was conducted at the

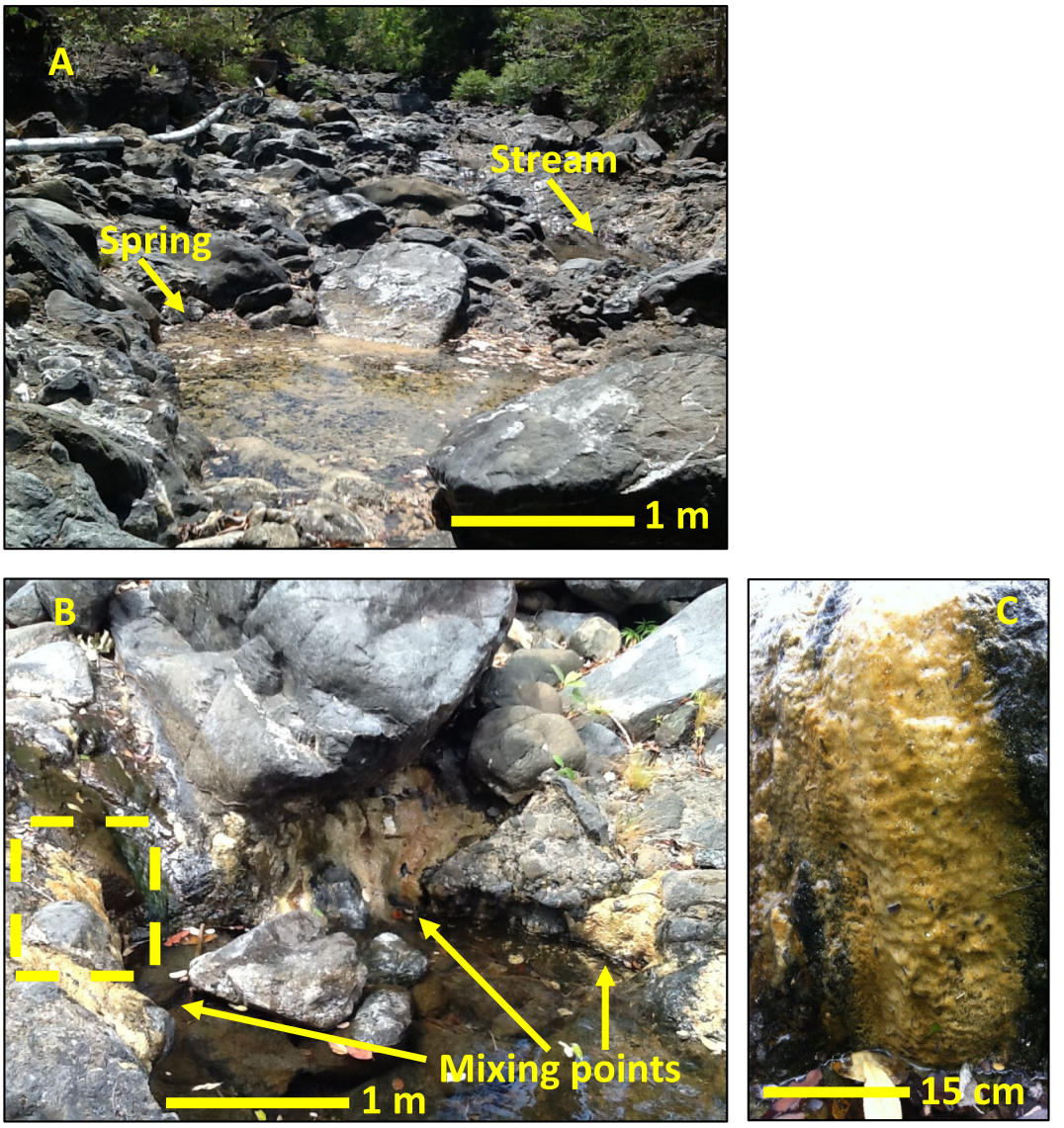

Figure 3. (a) Image of the hyperalkaline spring at Río Murciélago site showing pool on the right stream bank with presence of yellow-brown precipitates. (b) Image of yellow-brown precipitates covering riparian bedrocks and mixing points of hyperalkaline fluids and stream water. Dilution with receving stream water occurs rapidly. (c) Enlargement of yellow dashed-square area in Figure 3b. Preciptates in contact with stream water.

Chemistry School of the National University of Costa Rica using a cavity ring down spectroscopy (CRDS) water isotope analyzer (L2120-i, Picarro Inc.) following the methods described by *Lis et al.* [2008]. Laboratory standards, previously calibrated to the VSMOW2-SLAP2 reference waters were EAG ($\delta^2H = -255.0‰$, $\delta^{18}O = -30.8‰$), CAS ($\delta^2H = -64.2.3‰$, $\delta^{18}O = -8.3‰$), and DDI ($\delta^2H = -15.4‰$, $\delta^{18}O = -125.5‰$). EAG and CAS were used to normalize the results to the VSMOW2-SLAP2 scale, while DDI was a quality control standard. The laboratory precision for this analytical run was $\pm 0.5‰$ (1σ) for δ^2H and $\pm 0.1‰$ (1σ) for $\delta^{18}O$.

3.2. Gas Chemistry

Preliminary sampling revealed novel information about the presence of methane emissions within the Santa Elena Ophiolite. A gas vent located approximately 300 m upstream from the hyperalkaline system within the Poza del General (supporting information Table S1) was sampled for methane determinations. Gas emission occurred in nonuniform time intervals at the bottom of a 4 m deep pool. The streambed was surveyed to discard the presence of decomposing organic matter. Samples were collected using a 15.24 cm (diameter) HDPE funnel connected to a Supel-inert film gas sampling bag (3 mm thickness, Sigma-Aldrich)

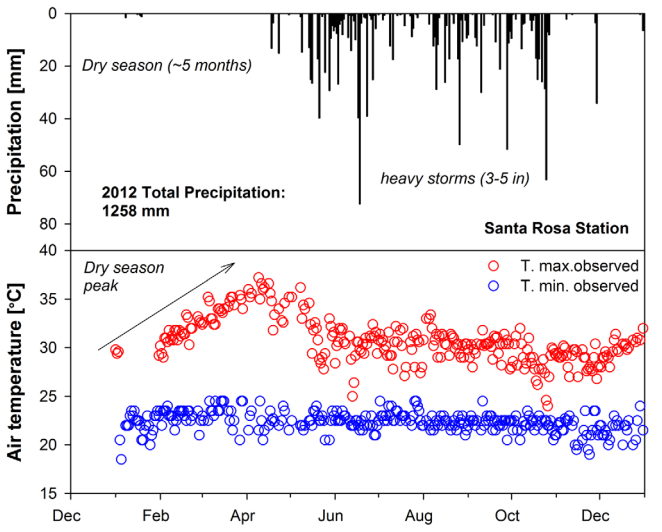

Figure 4. Santa Elena climate generalities. (top) Daily precipitation (mm). (bottom) Maximum and minimum ambient temperatures (°C) during the 2012 water year. Maximum temperature (April) is close to 40°C. Minimum temperature is on average 23°C.

through a 6 m long vinyl tubing (0.64 cm diameter) with a push-lock valve. The funnel was placed at the streambed by a professional diver to trap gas emanations. Three replicates were collected with a collection time of 20 min each.

Samples were analyzed within 4 days of collection at LAQAT Atmospheric Chemistry Laboratory (National University, Costa Rica) using a gas chromatographer (8610C, SRI Instruments) with a flame ionization detector; 1 mL of sample was injected with an automatic valve (Valco Instruments) into a 1 m column (Hayesep D, 0.32 cm diameter). Calibration was conducted with a methane standard (1% volume) (Scott Specialty Gases). Only methane was analyzed during these field explorations.

3.3. Carbonate Mineral Precipitates

Carbonate deposits and carbonate-bearing sediments underlying the deposits were collected at various locations within the riverbeds of the alkaline springs. At two springs (Murciélago and Potrero Grande, locations in supporting information Table S1), carbonate precipitates floating on the river water were sampled. Carbonate-bearing sediments and carbonate travertine deposits were crushed with the agate mortar to prepare bulk rock samples, while for a few travertine deposits single carbonate layers of the deposit were extracted with a 5 mm drill with the aim to reveal isotopic heterogeneities between different carbonate layers. The carbonate precipitates from the rivers were dried for 2 days at 40°C. All carbonate samples were in a final step homogenized to produce a fine-grained powder.

The mineralogy of the carbonate samples was determined by X-ray diffraction on a Rigaku MiniFlex XRD with powder diffraction analysis package PDXL at the Geosciences department at Virginia Tech. The carbon and oxygen isotope composition was analyzed on a MultiFlowGeo headspace sampler at Virginia Tech. Samples were prepared in septum vials, flushed with He, acidified with phosphoric acid and reacted for at least 3 h before analyses, as no magnesite or dolomite was present in any of the analyzed samples. Reproducibility is better than $\pm 0.1‰$ for $\delta^{13}C$ and better than $\pm 0.3‰$ for $\delta^{18}O$.

3.4. Microbiology

Fluid samples, ranging from 20 to 170 mL, were collected from the two alkaline springs at Río Murciélago (Spring 8 and Spring 9, Table S1) and from Quebrada Danta Spring and stored frozen until analyses. In the laboratory, samples were thawed and either preserved in 3.7% formaldehyde for cell counts and stored at 4°C, or filtered using sterile syringes through 0.2 μm Sterivex filter cartridges (Millipore) for DNA extraction. Fluids preserved for cell abundance enumeration were filtered through a 0.2 μm filter, and cells stained with 4′,6-diamidino were filtered counted with an Olympus BX61 spinning disk epifluorescence confocal microscope according to published protocols [*Hobbie et al*., 1977; *Schrenk et al*., 2003]. DNA extraction followed described protocols in *Huber et al*. [2002] and *Sogin et al*. [2006]. DNA extracts were purified with the DNA Clean and Concentrator™-5 kit (Zymo Research) according to the manufacturer's instructions.

16S rRNA amplicons (tag) were generated at the Marine Biological Laboratory (Woods Hole, MA) using an Illumina MiSeq apparatus. This method produces ~250 nt reads targeting the Bacterial and Archaeal 16S rRNA v4v5 region. Additional amplification and sequencing methods are available at the VAMPS website

Table 1. Percent of Sequences Related to Hydrogen, Methane, and Methanol Metabolism

Division	Family; Genus	Metabolism	Murciélago Spring 8	Murciélago Spring 9	Danta Spring
Bacteria	Pseudonocardiaceae; Pseudonocardia	Hydrogen oxidation	0.00	0.00	0.01
Bacteria	Hyphomicrobiaceae; Xanthobacter	Hydrogen oxidation	0.00	0.00	0.01
Bacteria	Hydrogenophilaceae; Hydrogenophilus	Hydrogen oxidation	0.24	0.01	0.00
Bacteria	Hydrogenophilaceae; Tepidiphilus	Hydrogen oxidation	0.00	0.14	0.00
Bacteria	Hydrogenophilaceae; Thiobacillus	Hydrogen oxidation	0.02	0.00	0.00
Bacteria	Rhodobacteraceae; Paracoccus	Hydrogen oxidation	0.18	0.02	0.00
Bacteria	Comamonadaceae; Azohydromonas	Hydrogen oxidation	0.00	0.00	0.00
Bacteria	Comamonadaceae; Hydrogenophaga	Hydrogen oxidation	8.10	19.82	3.21
Bacteria	Methylococcaceae; Methylocaldum	Methane oxidation	0.00	0.00	0.00
Bacteria	Methylococcaceae; Methylomonas	Methane oxidation	0.02	0.01	0.00
Bacteria	Methylococcaceae; Methylosoma	Methane oxidation	0.01	0.00	0.00
Bacteria	Methylobacteriaceae; Meganema	Methane oxidation	0.12	0.00	0.00
Bacteria	Methylobacteriaceae; Methylobacterium	Methane oxidation	0.26	0.01	0.01
Bacteria	Methylocystaceae; Methylocystis	Methane oxidation	0.08	0.01	0.00
Bacteria	Methylocystaceae; genus_NA[a]	Methane oxidation	0.59	0.00	0.00
Bacteria	Comamonadaceae; Methylibium	Methanol oxidation	49.64	1.36	0.70
Bacteria	Methylophilaceae; Methylophilus	Methanol oxidation	0.00	0.01	0.01
Bacteria	Methylophilaceae; Methylotenera	Methanol oxidation	0.00	0.01	0.00
Bacteria	Methylophilaceae; genus_NA	Methanol oxidation	0.00	1.42	1.09
Archaea	Methanobacteriaceae; Methanobacterium	Methanogenesis	0.46	0.83	0.14
Archaea	Methanobacteriaceae; Methanobrevibacter	Methanogenesis	0.00	0.53	0.00
Archaea	Methanobacteriaceae; genus_NA	Methanogenesis	0.00	3.75	28.87
Archaea	Methanocellaceae; Methanocella	Methanogenesis	0.00	0.00	0.00
Archaea	Methanocellaceae; Rice_Cluster_I	Methanogenesis	1.29	4.51	0.00
Archaea	Methanospirillaceae; Methanospirillum	Methanogenesis	0.01	6.79	0.00
Archaea	Methanosaetaceae; Methanosaeta	Methanogenesis	0.00	0.01	0.00

[a]NA = unclassified.

(http://vamps.mbl.edu/resources/primers.php). Data processing, chimera detection, and taxonomic classification procedures have been previously described [*Sogin et al*., 2006; *Huse et al*., 2008, 2010].

4. Results

Supporting information Table S1 presents a description of the sampling locations during both field expeditions (January and March 2013). Locations are described by their local name, sampling date and time, type of discharge, geographic coordinates (decimal degrees), and altitude (m). Supporting information Tables S2 and S3 contain physical parameters, stable isotopes, major ions, trace elements, and extended alkalinity composition of the surface, spring, and groundwaters collected in both sampling campaigns. Table 1 presents percent of sequences related to hydrogen, methane, and methanol metabolism in Río Murciélago Spring 8 and Spring 9, and Quebrada Danta spring (supporting information Table S1). Supporting information Table S4 presents Bacterial and Archaeal diversity by next-generation tag sequencing of the 16S rRNA gene. Supporting information Tables S5 and S6 contain information on the taxonomic classification of Bacterial and Archaeal tag sequences, respectively, that accounted for 1% or more of the total sequences in a sample.

4.1. Hyperalkaline Spring Systems

Potential hydrogen (pH) of the springs ranged from 11.01 up to 11.18 (Figure 5). Both spring systems, Murciélago and Potrero Grande (Figure 1), are representative of Ca^{2+}-OH^{-} waters. Hydroxide and carbonate concentrations ranged from 41 to 63 and 31 to 49 mg/L (reported as mg/L $CaCO_3$ equivalent), respectively. Maximum dissolved calcium concentrations of 167 mg/L were measured in Murciélago Spring 9 (supporting information Table S1). In addition, the springs are characterized by low Mg (1.0–5.9 mg/L) and K (1.0–5.2 mg/L) concentrations and relatively high Na (16–27 mg/L) and Cl (26–29 mg/L) (Figure 5). Nickel (15.5 μg/L) and iron (0.24 mg/L) were also measured in minor concentrations. Sulfate was not detected in the analyzed fluids (detection limit = 0.33 mg/L). Average spring temperature was 29 ± 2 (1σ)°C, which is 3°C higher than the average temperature of nonalkaline springs. Active gas vents with

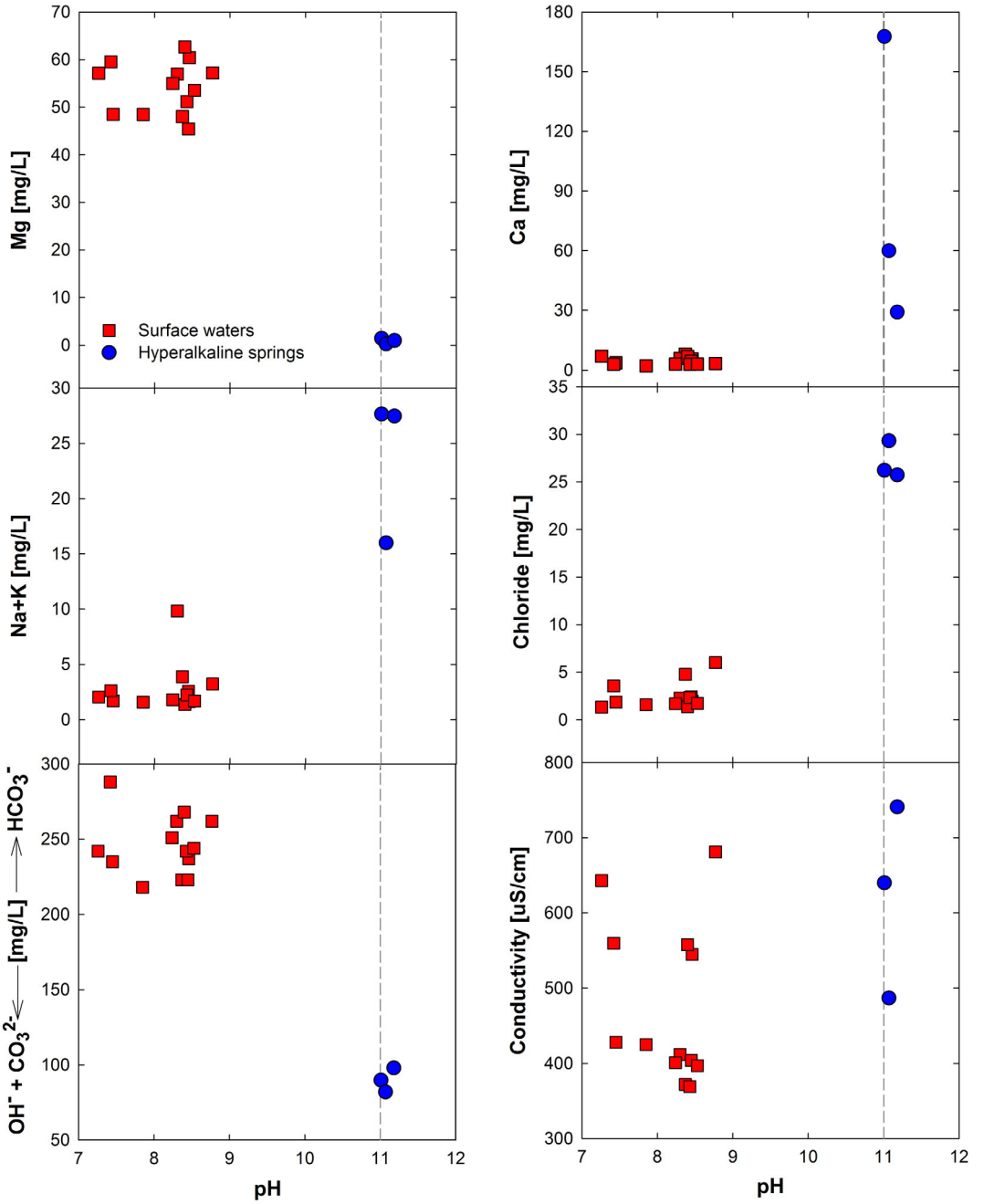

Figure 5. Surface water and hyperalkaline spring water chemical composition. Gray dashed line represents pH = 11.0. Hyperalkaline fluids are characterized by high Ca, Na + K, and chloride concentrations while surface waters show an inverse composition dominated by Mg and bicarbonate. Hydroxide and carbonate were only detected within the hyperalkaline springs.

CH_4 concentrations of up to 24.3% (v/v) were detected at the Río Murciélago site ~300 m upstream of the hyperalkaline spring system.

Hydrological connectivity between the groundwater system and hyperalkaline spring seepage was explored using stable isotopes in private and municipal wells. Isotope compositions of hyperalkaline fluids ($\delta^{18}O = -7.9‰$, $\delta^{2}H = -51.4‰$, Figure 6 and supporting information Table S3) are remarkably similar to the well signals ($\delta^{18}O = -7.6‰$; $\delta^{2}H = -48.0‰$) sampled within the Cuajiniquil and Murciélago watersheds. Isotopic base flow composition generally represents the mean annual isotopic composition of meteoric waters. In Costa Rica, the annual weighted precipitation composition is

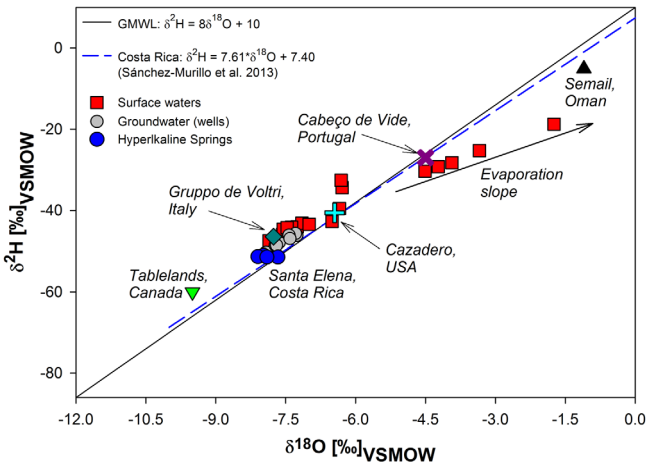

Figure 6. Stable isotope ($\delta^{18}O$ and δ^2H) composition (‰) of surface water (red squares), groundwater wells (gray circles), and hyperalkaline springs (blue circles) in the Santa Elena Ophiolite. Surface water samples follow an evaporation enrichment line as travel distance increases. Hyperalkaline springs show a similar isotopic signature compared with groundwater samples from 12 deep wells. Global and Costa Rica meteoric water lines are included to reference meteoric water origin. Mean stable isotope composition in similar subtropical and temperate locations are color coded: Hahwalah Wadi Jizi, Samail, Oman (black triangle) [*Barnes et al.*, 1978]; Cazadero, California, USA (cyan cross) [*Barnes et al.*, 1978]; Cabeço de Vide, Portugal (purple cross) [*Marques et al.*, 2008]; Tablelands, Gros Morne National Park, Canada (green triangle down) [*Szponar et al.*, 2012]; Gruppo di Voltri, Italy (dark green rhombus) [*Cipolli et al.*, 2004].

$\delta^{18}O = -7.4‰$ and $\delta^2H = -49‰$ [*Sánchez-Murillo et al.*, 2013] which corresponds to the isotopic signal found in the hyperalkaline fluids. Mean electrical conductivity (EC) in the hyperalkaline springs ranged from 487 up to 741 μS/cm.

4.2. Surface Waters

Well-mixed surface waters within the Santa Elena Peninsula are of a dominant Mg-bicarbonate system which represents ~95% of the major ions composition. Bicarbonate concentration ranges from 218 to 288 mg/L (i.e., reported as mg/L $CaCO_3$ equivalent) with a mean of 246 ± 20 (1σ) mg/L. Magnesium concentrations vary from 45 to 63 mg/L with a mean of 54 ± 5 (1σ) mg/L. Inversely to the hyperalkaline fluids, these surface waters showed low Ca 4.6 ± 5 mg/L (1σ), Na + K (1.4–9.8 mg/L) and chloride 2.5 ± 1.4 (1σ) mg/L concentrations (Figure 5). Mean surface water pH was 8.0 ± 0.5 (1σ); nevertheless, pH values greater than 8.5 were consistently measured across the studied streams (Figure 5). Electrical conductivity was on average 477 ± 107 (1σ) μS/cm across the main four watersheds. Surface water temperature was fairly uniform with a mean of 26.8 ± 1.4°C (1σ) across the studied streams. Mean isotope composition of surface waters ($\delta^{18}O = -6.8‰$, $\delta^2H = -43.4‰$) shows clear evaporation enrichment as traveltime increases from headwaters to the lower reach of the catchments (Figure 6).

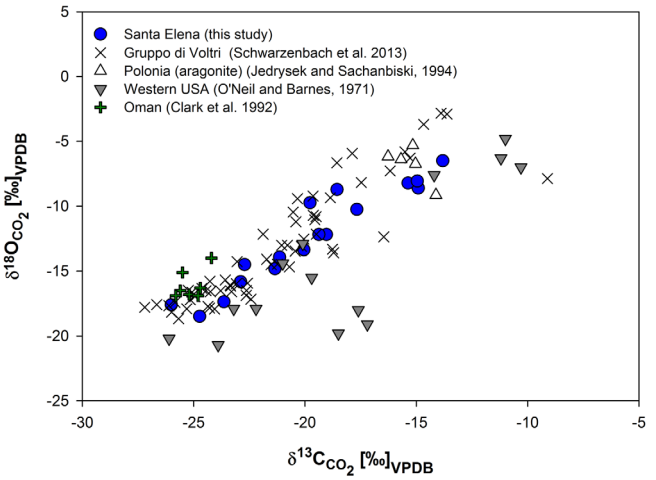

Figure 7. Comparison of Santa Elena $\delta^{13}C$ and $\delta^{18}O$ composition (‰) (blue circles) and summary of similar ultramafic hosted carbonate deposits in subtropical and temperate sites: Gruppo di Voltri, Italy (black crosses) [*Schwarzenbach et al.*, 2013b]; Polonia (open triangles) [*Jedrysek and Sachanbiski*, 1994]; Western USA (gray triangles down) [*O'Neil and Barnes*, 1971]; Oman (green crosses) [*Clark et al.*, 1990]. Santa Elena's carbon and oxygen isotope composition of carbonates is within the range of similar ultramafic hosted carbonate deposits.

4.3. Groundwater

Groundwater EC ranged from 504 to 1084 μS/cm with a mean of 722 ± 220 (1σ) μS/cm, which is 1.2 and 1.5 times greater than hyperalkaline springs and surface waters, respectively, which indicates a greater extent of water-rock interaction. Mean well water temperature was 30 ± 2°C (1σ). One sample from well Aguas Calientes (supporting information Table S3) was analyzed for aqueous chemistry. Interestingly, this well is located outside the ophiolite; however, the headwaters of Cuajiniquil watershed are within the peridotite. Besides the pH (7.2), the composition of this well water shared similarities with alkaline fluids: high Ca (73 mg/L), sulfate (5.74 mg/L), Cl (41.3 mg/

L), Na (16.2 mg/L), low Mg (4.33 mg/L), and Fe (1.35 mg/L), which may indicate that deep percolation is also transferring the hyperalkaline signature to the groundwater system. As mentioned in section 4.1, groundwater isotope composition was remarkably similar to hyperalkaline fluids.

4.4. Carbonate Deposits

Strongly ^{13}C and ^{18}O depleted calcite deposits suggest calcite precipitation by uptake of atmospheric CO_2 dominated by kinetic fractionation and are found in many continental serpentinization systems (Figure 7) [*Clark et al*., 1990; *O'Neil and Barnes*, 1971; *Schwarzenbach et al*., 2013b; *Quesnel et al*., 2013]. These characteristically depleted isotope compositions are a result of the high pH and extremely low C_{total} of the fluids, which causes immediate uptake of CO_2 upon interaction with the atmosphere. With continuous interaction of the fluids with the atmospheric CO_2, the formed carbonates get less negative in their isotopic composition resulting in the linear trend seen in Figure 6. This process has been described in detail for ^{13}C and ^{18}O depleted calcite deposits in the Voltri Massif, Italy [*Schwarzenbach et al*., 2013b] (Figure 7).

4.5. Microbiology

Quebrada Danta spring had the highest cell density (1.51×10^5 cells/mL). Cell densities at Río Murciélago Spring 8 and Spring 9 were 7.93×10^4 and 2.0×10^4 cells/mL, respectively. These values reflect low biomass, which is consistent with other serpentinizing systems. Bacterial and Archaeal diversity were estimated by next-generation tag sequencing of the 16S rRNA gene (supporting information Table S4).

Evidence of microorganisms involved in hydrogen oxidation, methane, and methanol oxidation, as well as methananogenesis can be deduced from our sequencing results (Table 1). Sequences related to methanotrophs belonging to the families *Methylococcaceae*, *Methylobacteriaceae*, and *Methylocystaceae* were found in all samples, being more abundant at Río Murciélago Spring 8. The bacterial community in this spring was highly dominated by the genus of methylotrophic bacteria *Methylibium* (50% of the total sequences in this sample). Although to a lesser extent, sequences related to several genera within the family of methanol oxidizers *Methylophilaceae* were identified in Río Murciélago Spring 9 and Quebrada Danta sample (supporting information Table S1). Two genera dominated the community in Murciélago Spring 9; the alkaliphilic genera *Silanimonas* and the H_2-oxidizing genus *Hydrogenophaga*. Representatives of these genera have been previously detected at other surveys from other continental serpentinite springs [*Brazelton et al*., 2013; *Susuki et al*., 2013]. *Hydrogenophaga* sequences were identified in all samples, as well as other hydrogen oxidizing bacteria from the families *Hydrogenophilaceae*, *Hyphomicrobiaceae*, *Pseudonocardiaceae*, and *Rhodobacteraceae*.

Signatures of methanogenic archaea from the orders *Methanobacteriales*, *Methanocellales*, and *Methanomicrobiales* were detected in all samples (Table 1) suggesting methanogenesis as an important process at this system, as has been suggested for other serpentinizing environments [*Blank et al*., 2009; *Brazelton et al*., 2012; *Susuki et al*., 2013]. This initial community composition analyses indicate the presence of microorganisms typically associated with other serpentinizing environments; however, additional sequence data as well as activity and transcriptomic data would further expand our knowledge of the microbial communities thriving this system and their metabolism.

5. Discussion

5.1. Serpentinization and Hydrology: The Role of a Tropical Environment

In the tropics, base flow can be seen as the cumulative outflow from all upstream riparian areas (i.e., adjacent areas along the stream channel) and deep aquifers during rainless periods; its discharge (e.g., spring seepage or gaining streams) regulates stream chemistry and water temperature during critical dry months. The natural release of water as base flow can be seen as a function of the hydraulic properties within the underlying geology and climatic conditions [*Brutsaert*, 2005]. From a hydrological perspective, underlying geologic features are invariant with time (decades to hundreds of years) and significant climate effects can be distinguished only over large timeframes. However, hydrological processes in ophiolites, particularly, infiltration and groundwater flow are permanently altered due to active serpentinization resulting in constant volume changes in the altered materials [*Macdonald and Fyfe*, 1985; *Shervais et al*., 2005; *Schrenk et al*., 2013]; these transformations may play a key role in the overall subsurface flow paths distribution.

This novel hydrogeological system invokes three fundamental questions: (a) To what extent can serpentinization and microbial life be facilitated in a humid environment under high infiltration rates during the rainy season?, (b) How do subsurface water-rock interaction pathways and mean transit time influence spring water geochemistry?, and (c) What are the effects on the system effective porosity and hydraulic conductivity and overall solute transport by carbonate precipitates related with the serpentinization process? A humid serpentinizing environment with high meteoric water infiltration—as expected in the Santa Elena Ophiolite—may stimulate the growth of microbial communities by replenishing oxidants and nutrients (i.e., including carbon) in the shallow subsurface flow paths while benefiting from accelerated rates of water-rock reaction and associated hydrogen and methane evolution. The mean transit time or (MTT) the time a water molecule or solute spends traveling along subsurface flow pathways to the stream network is a fundamental hydraulic descriptor that provides useful information about water sources and mixing processes, potential flow pathways, and storage capabilities within a particular catchment control volume [*McGuire et al*., 2002; *Dunn et al*., 2007; *Soulsby et al*., 2009; *Stewart et al*., 2012; *Sanghyun and Sungwon*, 2014]. However, despite its relevance, mean transit time has been poorly investigated in continental serpentinization studies [*Dewandel et al*., 2005]. Detailed description of MTT coupled with geochemical data from alkaline seepage could provide a quantitative descriptor of water-rock contact time. Likewise, the dissolution and precipitation of minerals along the subsurface flow paths could alter the aquifer effective porosity, and consequently, the hydraulic conductivity of the system. In the case of the Santa Elena Ophiolite, the high variability of precipitation events during the wet season (May–November) (Figure 4) may concatenate changes in hydraulic conductivity (i.e., horizontal and vertical anisotropy) across a geological setting with mostly less than 50% degree of serpentinization.

Figure 8 shows a schematic rationale of water flow paths coupled with base flow geochemical evidence. In the Santa Elena Ophiolite, base flow conditions comprise approximately 4–5 months of the streamflow regime in which the minimum discharge occurs late in April or the beginning of May; it is clear that the peridotite-aquifer storativity is large enough to maintain base flow in Potrero Grande and Murciélago after prolonged dry periods.

Due to the absence of a well-developed soil profile (less than 20 cm), infiltration of meteoric water occurs directly through the ultramafic rocks. Consequently, infiltrated water is modified by the serpentinization process before discharging at a topographic low (Figure 8). Once at the surface, hyperalkaline fluid chemistry is modified by evaporation, precipitation, and mixing processes. Meteoric water can also flow through fully serpertinized macropores (e.g., faults) preserving a near neutral pH (∼7.2) and freshwater-type chemistry characteristics if the system is open in respect to CO_2. Near neutral pH values may also correspond to short residence times in some of these springs. This type of spring is common and can be found in the proximity of hyperalkaline seepages, which supports the hypothesis of an intricate anisotropic subsurface matrix. Perennial surface waters exhibited slightly alkaline conditions (pH 8.0–8.7) due to the potential mixing with serpentinizing fluids along the stream reach (Figure 8), such as diffuse bank sources. Despite high surface runoff and evapotranspiration amounts, rivers such as the Potrero Grande, Cuajiniquil, and Murciélago (Figure 1) are perennial in most of their main sections. Perennial discharge suggests a large water storativity in the mantle peridotite and a higher hydraulic head in the peridotite than in the perennial streams. The groundwater system is most likely an unconfined aquifer underlain by a basalt impermeable layer at the base of the ophiolite overthrust or between basaltic sills as observed during the field expeditions. Based on the *Mulligan and Burke* [2005] regionalized hydrological model, recharge may represent 18% of the available precipitation, whereas runoff may reach as much as 21%.

Dewandel et al. [2003, 2004, 2005] studied the base flow response within a similar ultramafic formation in Oman. Although Oman is located in a subtropical arid region with precipitation amounts of approximately 250 mm/yr, the hydraulic peridotite properties may share strong similarities. The authors found that in ophiolite rocks, groundwater circulation takes place mostly in the fissures close to the surface horizon (∼50 m), and, to a lesser degree, in the tectonic fractures. In a water year of 250 mm available precipitation, *Dewandel et al*. [2005] estimated that only 8% (20 mm/yr) contributed to groundwater recharge, 12% runoff (30 mm/yr), and 80% evapotranspiration (200 mm/yr). Hydraulic conductivity of the fissured horizon was estimated at 10^{-5} to 10^{-6} m/s for gabbro and diabase, and 10^{-7} m/s for peridotite. In general, the authors concluded that despite low annual rainfall, a relatively low hydraulic conductivity and a significant storage coefficient explain the perennial behavior of the streams within the peridotite. *Dewandel et al*. [2005] also

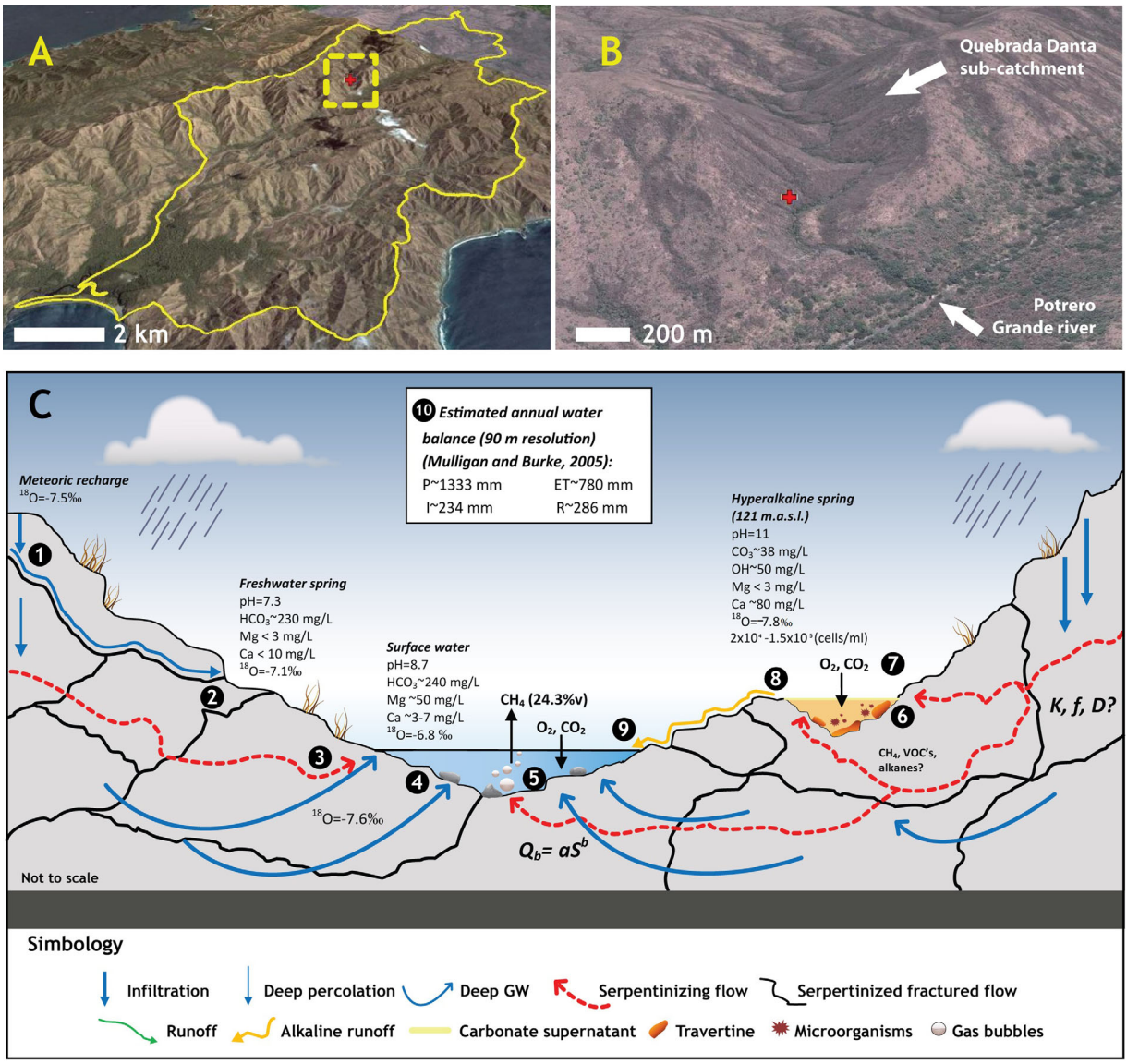

Figure 8. Schematic representation illustrating the hyperalkaline base flow process proposed for the Santa Elena Ophiolite. (a) Digital elevation overview of Potrero Grande watershed (Landsat Image, USGS, 90 m). Yellow line represents watershed boundary and yellow dashed-square denotes Quebrada Danta subcatchment. Red cross corresponds to the hyperalkaline system. (b) Enlargement of yellow dashed-square area over Quebrada Danta subcatchment; mean basin slope is ~33%. Vegetation is scarce on hillslopes; but mostly concentrated in the riparian zones of the floodplain. (c) A conceptual hyperalkaline base flow process coupled with measured water chemistry and field observations. Soil profile is relatively absent (less than 20 cm). Infiltration occurs directly through the ultramafic formation (1). Piston-type flow may occur within serpertinized fractured macropores (i.e., faults) producing freshwater springs if the system is open in respect to CO_2 (2). These flow paths appear to be relatively shallow. Deep groundwater flow feeds the creek during the dry season (4). Base flow discharge is a function of storage, where *a* corresponds to the characteristic recession time scale (presumably low due to high evapotranspiration). Hydraulic parameters such as conductivity (K), drainage porosity (*f*), and aquifer thickness (*D*) are unknown. If the system responds as a linear reservoir, then $b = 1$. Deep groundwater flow may dilute the signature of active serpentinizing (3). However, active serpentinizing flow paths could also emerge as hyperalkaline springs probably with an exponential-piston flow distribution due to the constant structural changes (6). Hyperalkaline fluids form riparian pools coated by a $CaCO_3$ supernatant film where travertine terraces are evident and potential heterotrophic microbial methanogenesis may also occur (7 and 8). The hyperalkaline fluids are characterized by high pH, Ca, and low Mg. The fluids mix with receiving stream waters at low rates and volumes, thus, dilution occurs rapidly (9). As measured in the Río Murciélago watershed methane emanations (24.3% v/v) occur at the streambed (5). Other hydrocarbons may be produced during the serpentinization process. Based on the *Mulligan and Burke* [2005] regional hydrological model (90 m resolution), recharge could be approximately 18% of the water budget whereas runoff could reach up to 21% during the wet season and evapotranspiration is roughly 60%. Shallow storage could be as lower as 3%.

illustrated a deep circulation (~500 m deep) with a residence time up to 25 years as a common subsurface flow mode, requiring high potential energy to allow for deep-circulation flow paths; resulting in spring flow near or in mountain areas. Another study conducted by *Matter et al.* [2006] also provided valuable hydraulic information of the Samail Ophiolite. For instance, the authors reported transmissivities ranging from 8×10^{-5} to 1×10^{-4} m^2/s and an average storage coefficient of 8×10^{-4} within fractured and weathered

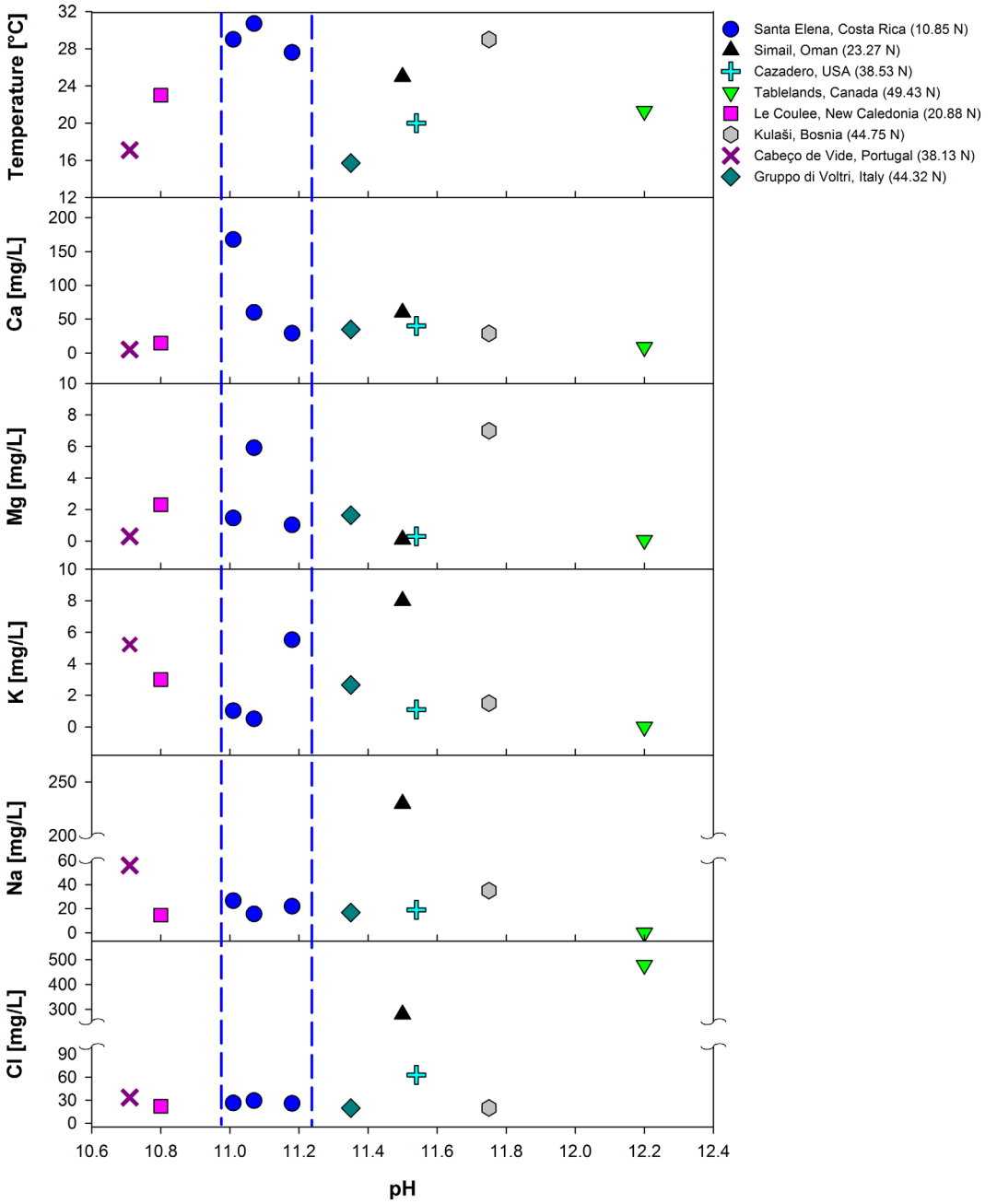

Figure 9. Comparison of Santa Elena aqueous geochemistry and mean composition of hyperalkaline springs in similar subtropical and temperate locations: Hahwalah Wadi Jizi, Samail, Oman [*Barnes et al.*, 1978]; Cazadero, California, USA [*Barnes et al.*, 1978]; Le Coulee 1, New Caledonia [*Barnes et al.*, 1978]; Kulaši, Bosnia [*Barnes et al.*, 1978]; Cabeço de Vide, Portugal [*Marques et al.*, 2008]; Tablelands, Gros Morne National Park, Canada [*Szponar et al.*, 2012]; Gruppo di Voltri, Italy [*Cipolli et al.*, 2004]. Numbers in parentheses denote latitude in decimal degrees. Blue dashed-lines emphasize Santa Elena lower and upper pH limits.

peridotites. *Matter et al.* [2006] also suggested that fracturing during tectonic emplacement and consequently weathering produced an increase of near-surface porosity.

Water supply during the wet season sets the Santa Elena Ophiolite apart from the hydrological scenarios observed in temperate or semiarid regions. The potential of meteoric recharge can be analyzed from two perspectives: annual rainfall amounts and individual storm size. In Santa Elena, daily rainfall amounts can reach up to 211 mm (based on 10 years of historical records at the Santa Rosa climatological station, supporting information Figure S1); this is approximately equal to the annual precipitation in Oman (supporting information Figure S2). In Newfoundland, Canada, and Genoa, Italy, daily precipitation amounts (based on

20 years of historical records, National Climate Data Center [2013]; supporting information Figure S2) can reach up to 94 and 154 mm, respectively. Although mean annual precipitation amounts in Genoa, Italy (1135 mm) and Newfoundland, Canada (1108 mm) are close to Santa Elena's annual precipitation (1434 mm); what makes Santa Elena so unique is that the water supply is received in only 6 months rather than intermittent rainfall activity or snowpack accumulation. For example, meteoric recharge in Santa Elena is on average 10 times greater than those reported in Oman [*Dewandel et al*., 2005]; that being the case, it is plausible to expect that fissuring and constant development of macropores flow or active lateral flow pathways may increase to a great extent the permeability (i.e., vertically and horizontally) in the peridotite resulting in greater water-rock interaction during the wet season and hyperalkaline fluid seepage throughout the base flow period.

5.2. Hyperalkaline Fluid Chemistry Comparison With Other Ultramafic Systems

Figure 9 shows a comparison of hyperalkaline fluid composition in multiple ultramafic systems in temperate (Gruppo di Voltri, Italy; Cabeço de Vide, Portugal; Tablelands, Canada; Cazadero, USA; Kulasi, Bosnia), subtropical (Samail, Oman), and tropical environments (Le Coulee, New Caledonia; Santa Elena, Costa Rica, this study). As expected in a tropical setting, Santa Elena's hyperalkaline fluids exhibited the highest water temperature (29.0–30.7°C) compared to the other sites. Recently, *Chavagnac et al*. [2013] reported temperatures ranging from 33 to 40°C in the Oman Ophiolite; yet these high temperatures are mostly the result of radiative heating of the surface waters. The lowest spring temperatures (below 18°C) correspond to the Gruppo di Voltri, Italy and Cabeço de Vide, Portugal. Overall, spring temperatures among all sites support the idea of an internal heat source related to present-day continental serpentinization. Calcium concentrations appear to be consistently between 5.1 and 60 mg/L; however, in this study, Spring 9 in the Murciélago River has a maximum value of 167 mg/L, which may be evidence of active serpentinization rate versus a low CO_2 uptake. *Palandri and Reed* [2004] reported that serpentinizing waters may export high dissolved Ca concentrations out of the system, thus, if this solute transport process is slower than the CO_2 uptake (i.e., in a system that is closed in respect to CO_2) [*Bruni et al*., 2002] then Ca can accumulate in the hyperalkaline seepage pools. All ultramafic systems are consistently depleted in Mg concentrations. Depletion of Mg can be explained by formation of serpentine and/or brucite as suggested by *Bruni et al*. [2002]:

$$Mg^{2+}(aq) + 2\ OH^{-} = Mg(OH)_2(s) \quad \text{(R1)}$$

$$3\ Mg^{2+}(aq) + 2SiO_2(aq) + 5H_2O = 2Mg_3Si_2O_5(OH)_4(s) + H^{+} \quad \text{(R2)}$$

Other element chemistry such as Na, K, and Cl are within very similar ranges, except for the springs in the Oman Ophiolite where saltier conditions result in greater concentrations.

6. Conclusions

Field explorations in the Santa Elena Ophiolite provide strong evidence of active serpentinization in the area. In the hyperalkaline fluids, Mg was highly depleted probably due to serpentine formation and brucite precipitation in the subsurface, whereas Ca was abundant along with high concentrations of hydroxide, carbonates, and chloride. Further, the combination of active methane vents and extensive carbonate deposits also provide evidence of active serpentinization, though, methane may also form through methanogenic organisms. Signatures of methanogenic archaea from the orders *Methanobacteriales*, *Methanocellales*, and *Methanomicrobiales* detected in the hyperalkaline fluids suggest that methanogenesis is an important process at this system. Further evidence for active serpentinization could give the possible presence of H_2 in the spring waters, which will be considered in future studies.

Natural well-mixed surface waters were characterized by a dominant $Mg-HCO_3^-$ system, which represents ~95% of the major ions composition. Stable isotope data show notable groundwater to surface water connectivity in the main perennial rivers where the hyperalkaline fluids were discovered. Most importantly, spring seepage temperature and isotopic composition (i.e., plotted on the local meteoric water line) strongly suggest no isotopic enrichment or any external heat source such as hydrothermal activity.

Overall, the long rainy season coupled with high rainfall intensity mainly controlled by coastal convective storms position the Santa Elena Ophiolite as an analog of an early humid Earth where meteoric water inputs were abundant and mainly dominated by changes in the global circulation and sea surface temperature

regimes. Given the distribution of mafic-ultramafic rocks on other planetary environments (e.g., Mars), the unique Santa Elena's environment will serve as a natural laboratory to better and fully characterize the planetary conditions that can support life. Likewise, variations in the carbonate mineralogy of veins or layered deposits can give insight into changing fluid compositions and element transport that might be a result of seasonal changes in the hydrological cycle.

Future work on the of carbonate deposits formed by discharge of the hyperalkaline springs will serve to refine the search criterion for the surface expression of these systems which could be used to identify both active and inactive serpentinization systems on other planetary bodies. Further evaluations will require continuous physical-chemical monitoring (i.e., resolution of minutes to hours) coupled with sampling of hyperalkaline fluids on an event basis (i.e., single storm responses) to determine the role of rapid meteoric recharge in serpentinization rates and chemosynthetic organisms as well as depicting the evolution of the hyperalkaline fluids composition throughout the base flow recession regime.

Acknowledgments

The authors wish to thank the valuable collaboration from the ACG personnel, especially, Roger Blanco Segura (Research Program Coordinator), M. Marta Chavarría (Biodiversity especialist), and J. Calvo (field assistant). Field assistance by P. Madrigal and P. Denyer was also fundamental for field expeditions. We would like to thank the laboratory assistance of H. Hernández at Agrotec Analytical Laboratory and G. Esquivel, R. Alfaro, and J. Valdés at the Chemistry School of the National University, Costa Rica as well as figure designs by A. Alcocer at University of Idaho. Santa Rosa weather data were kindly provided by the ACG. We thank W. Bach and anonymous reviewers for helpful comments. This project was supported by the National Science Foundation grant EAR-1019327 to EG and from the Deep Carbon Observatory (Alfred P Sloan Foundation) grant to MOS.

References

Abrajano, T. A., N. C. Sturchio, J. K. Bohlke, G. L. Lyon, R. J. Poreda, and C. M. Stevens (1988), Methane-hydrogen gas seeps, Zambales ophiolite, Philippines: Deep or shallow origin?, *Chem. Geol.*, *71*, 211–222, doi:10.1016/0009-2541(88)90116-7.

Abrajano, T. A., N. C. Sturchio, B. M. Kennedy, and G. L. Lyon (1990), Geochemistry of reduced gas related to serpentinization of the Zambales ophiolite, Philippines, *Appl. Geochem.*, *5*, 625–630, doi:10.1016/0883-2927(90)90060-I.

Allen, D. E., and W. E. J. Seyfried (2003), Compositional controls on vent fluids from ultramafic-hosted hydrothermal systems at mid-ocean ridges: An experimental study at 400°C, 500 bars, *Geochim. Cosmochim. Acta*, *67*, 1531–1542, doi:10.1016/S0016-7037(02)01173-0.

Alt, J. C., W. C. Shanks, W. Bach, H. Paulick, C. J. Garrido, and G. Beaudoin (2007), Hydrothermal alteration and microbial sulfate reduction in peridotite and gabbro exposed by detachment faulting at the Mid-Atlantic Ridge, 15°20′N (ODP Leg 209): A sulfur and oxygen isotope study, *Geochem. Geophys. Geosyst.*, *8*, Q08002, doi:10.1029/2007GC001617.

Alt, J. C., E. M. Schwarzenbach, G. L. Früh-Green, W. C. Shanks, S. M. Bernasconi, C. J. Garrido, L. Crispini, L. Gaggero, J. A. Padrón-Navarta, and C. Marchesi (2013), The role of serpentinites in cycling of carbon and sulfur: Seafloor serpentinization and subdurction metamorphism, *Lithos*, *178*(15), 40–54, doi:10.1016/j.lithos.2012.12.006.

Bach, W., H. Paulick, C. J. Garrido, B. Ildefonse, W. P. Meurer, and S. E. Humphris (2006), Unraveling the sequence of serpentinization reactions: Petrography, mineral chemistry, and petrophysics of serpentinites from MAR 15°N (ODP Leg 209, Site 1274), *Geophys. Res. Lett.*, *33*, L13306, doi:10.1029/2006GL025681.

Barnes, I., V. C. LaMarceh, and G. Himmelberg (1967), Geochemical evidence of present-day serpentinization, *Science*, *156*, 830–832.

Barnes, I., J. R. O'Neil, and J. J. Trescases (1978), Present day serpentinization in New Caledonia, Oman and Yugoslavia, *Geochim. Cosmochim. Acta*, *42*, 144–145.

Barron, E. J., W. W. Hay, and S. Thompson (1989), The hydrologic cycle: A major variable during Earth history, *Global Planet. Change*, *1*(3), 157–174, doi:10.1016/0031-0182(89)90175-2.

Baumgartner, P. O., and P. Denyer (2006), Evidence for middle Cretaceous accretion at Santa Elena Peninsula (Santa Rosa Accretionary Complex), Costa Rica, *Geol. Acta*, *4*(1–2), 179–191.

Blank, J. G., S. J. Green, D. Blake, J. W. Valley, N. T. Kita, A. Treiman, and P. F. Dobson (2009), An alkaline spring system within the Del Puerto Ophiolite (California, USA): A Mars analog site, *Planet. Space Sci.*, *57*, 533–540, doi:10.1016/j.pss.2008.11.018.

Boschetti, T., and L. Toscani (2008), Springs and streams of the Taro-ceno valleys (northern Apennine, Italy): Reaction path modeling of waters interacting with serpentinized ultramafic rocks, *Chem. Geol.*, *257*, 76–91, doi:10.1016/j.chemgeo.2008.08.017.

Brazelton, W. J., M. O. Schrenk, D. S. Kelley, and J. A. Baross (2006), Methane- and sulfur-metabolizing microbial communities dominate the Lost City hydrothermal field ecosystem, *Appl. Environ. Microbiol.*, *72*(9), 6257–6270, doi:10.1128/AEM.00574-06.

Brazelton, W. J., M. L. Sogin, and J. A. Baross (2010), Multiple scales of diversification within natural populations of archaea in hydrothermal chimney biofilms, *Environ. Microbiol. Rep.*, *2*(2), 236–242, doi:10.1111/j.1758-2229.2009.00097.x.

Brazelton, W. J., B. Nelson, and M. O. Schrenk (2012), Metagenomic evidence for H_2 oxidation and H_2 production by serpentinite-hosted subsurface microbial communities, *Front. Microbiol.*, *2*, 268, doi:10.3389/fmicb.2011.00268.

Brazelton, W. J., P. L. Morrill, N. Szponar, and M. O. Schrenk (2013), Bacterial communities associated with subsurface geochemical processes in continental serpentinite springs, *Appl. Environ. Microbiol.*, *79*(13), 3906–3916, doi:10.1128/AEM.00330-13.

Bruni, J., M. Canepa, G. Chiodini, R. Cioni, F. Cipolli, A. Longinelli, L. Marini, G. Ottonello, and M. V. Zuccolini (2002), Irreversible water-rock mass transfer accompanying the generation of the neutral, Mg-HCO_3 and high-pH, Ca-OH spring waters of the Genova province, Italy, *Appl. Geochem.*, *17*, 455–474, doi:10.1016/S0883-2927(01)00113-5.

Brutsaert, W. (2005), *Hydrology: An Introduction*, 605 pp., Cambridge Univ. Press, Cambrigde, U. K.

Cannat, M. (1993), Emplacement of mantle rocks in the sea-floor at mid-ocean ridges, *J. Geophys. Res.*, *98*(B3), 4163–4172, doi:10.1029/92JB02221.

Cannat, M., F. Fontaine, and J. Escartín (2013), Serpentinization and associated hydrogen and methane fluxes at slow spreading ridges, in *Diversity of Hydrothermal Systems on Slow Spreading Ocean Ridges*, edited by P. A. Rona et al., AGU, Washington, D. C., doi:10.1029/2008GM000760.

Carr, M. J., I. Saginor, G. E. Alvarado, L. L. Bolge, F. N. Lindsay, K. Milidakis, B. D. Turrin, M. D. Feigenson, and C. C. Swisher (2007), Element fluxes from the volcanic front of Nicaragua and Costa Rica, *Geochem. Geophys. Geosyst.*, *8*, Q06001, doi:10.1029/2006GC001396.

Chavagnac, V., C. Monnin, G. Ceuleneer, C. Boulart, and G. Hoareau (2013), Characterization of hyperalkaline fluids produced by low-temperature serpentinization of mantle peridotites in the Oman and Liguria ophiolites, *Geochem. Geophys. Geosyst.*, *14*, 2496–2522, doi:10.1002/ggge.20147.

Christensen, P. R., Jr., et al. (2005), Evidence for magmatic evolution and diversity on Mars from infrared observations, *Nature*, *436*, 504–509, doi:10.1038/nature03639.

Cipolli, F., B. Gambardella, L. Marini, G. Ottonello, and M. V. Zuccolini (2004), Geochemistry of high-pH waters from serpentinites of the Gruppo di Voltri (Genova, Italy) and reaction path modeling of CO_2 sequestration in serpentinite aquifers, *Appl. Geochem.*, *19*, 787–802, doi:10.1016/j.apgeochem.2003.10.007.

Clark, I. D., and J. C. Fontes (1990), Paleoclimatic reconstrution in the nothern Oman based on carbaontes from hyperalkaline groundwaters, *Quat. Res.*, *33*(3), 320–336, doi:10.1016/0033-5894(90)90059-T.

Craddock, R., and A. Howard (2002), The case for rainfall on a warm, wet early Mars, *J. Geophys. Res.*, *107*(E11), 5111, doi:10.1029/2001JE001505.

Denyer, P., and E. Gazel (2009), The Costa Rican Jurassic to Miocene oceanic complexes: Origin, tectonics and relations, *J. South Am. Earth Sci.*, *28*(4), 429–442, doi:10.1016/j.jsames.2009.04.010.

Dewandel, B., P. Lachassagne, M. Bakalowicz, P. Weng, and A. Al-Malki (2003), Evaluation of aquifer thickness by analyzing recession hydrographs: Application to the Oman ophiolite hard-rock aquifer, *Hydrology*, *274*, 248–269, doi:10.1016/S0022-1694(02)00418-3.

Dewandel, B., P. Lachassagne, and A. Qatan (2004), Spatial measurements of stream baseflow, a relevant method for aquifer characterization and permeability evaluation: Application to a hard-rock aquifer, the Oman ophiolite, *Hydrol. Processes*, *18*, 3391–3400, doi:10.1002/hyp.1502.

Dewandel, B., P. Lachassagne, F. Boudier, S. Al-Hattali, B. Ladouche, J. L. Pinault, and Z. Al-Suleimani (2005), A conceptual hydrogeological model of ophiolite hard-rock aquifers in Oman based on a multiscale and a multidisciplinary approach, *Hydrogeology*, *13*, 708–726, doi:10.1007/s10040-005-0449.

Dunn, S. M., J. J. McDonnell, and K. B. Vaché (2007), Factors influencing the residence time of catchment waters: A virtual experiment approach, *Water Resour. Res.*, *43*, W06408, doi:10.1029/2006WR005393.

Eaton, A. D., L. S. Clesceri, A. E. Greenberg, and M. A. H. Franson (1998), *Standard Methods for the Examination of Water and Wastewater*, Am. Public Health Assoc., Washington, D. C.

Etiope, G., B. Tsikouras, S. Kordella, E. Ifandi, D. Christodoulou, and G. Papatheodorou (2013), Methane flux and origin in the Othrys ophiolite hyperalkaline springs, Greece, *Chem. Geol.*, *347*, 161–174, doi:10.1016/j.chemgeo.2013.04.003.

Fairén, A. (2010), A cold and wet Mars, *Icarus*, *208*, 165–175, doi:10.1016/j.icarus.2010.01.006.

Frost, B. R. (1985), On the stability of sulfides, oxides, and native metals in serpentinite, *J. Petrol.*, *26*, 31–63, doi:10.1093/petrology/26.1.31.

Frost, B. R., and J. S. Beard (2007), On silica activity and serpentinization, *J. Petrol.*, *48*, 1351–1368, doi:10.1093/petrology/egm021.

Früh-Green, G. L., J. A. Connelly, A. Plas, D. S. Kelley, and B. Grobéty (2004), Serpentinization of oceanic peridotites: Implications for geochemical cycles and biological activity, in *The Subseafloor Biospere at Mid-Ocean Ridges*, vol. 144, AGU, Washington D. C.

Gazel, E., P. Denyer, and P. O. Baumgartner (2006), Magmatic and geotectonic significance of Santa Elena Peninsula, Costa Rica, *Geol. Acta*, *4*(1–2), 193–202, doi:10.1344/105.000000365.

Guswa, A. J., A. Rhodes, and S. E. Newell (2007), Importance of orographic precipitation to the water resources of Monteverde, Costa Rica, *Adv. Water Resour.*, *30*, 2098–2112, doi:10.1016/j.advwatres.2006.07.008.

Hand, K. P., R. W. Carlson, and C. F. Chyba (2007), Energy, chemical disequilibrium, and geological constraints on Europa, *Astrobiology*, *7*, 1006–1022, doi:10.1089/ast.2007.0156.

Hauff, F., K. Hoernle, P. Van den Bogaard, G. E. Alvarado, and D. Garbe-Schönber (2000), Age and geochemistry of basaltic complexes in western Costa Rica: Contributions to the geotectonic evolution of Central America, *Geochem. Geophys. Geosyst.*, *1*(5), 1009, doi:10.1029/1999GC000020.

Herzberg, C., and E. Gazel (2009), Petrological evidence for secular cooling in the mantle plumes, *Nature*, *458*(7238), 619–622.

Hobbie, J. E., R. J. Daley, and S. Jasper (1977), Use of nucleopore filters for counting bacteria by fluorescence microscopy, *Appl. Environ. Microbiol.*, *33*, 1225–1228.

Hoefen, T. M., R. N. Clark, J. L. Bandfield, M. D. Smith, J. C. Pearl, and P. R. Christensen (2003), Discovery of olivine in the Nili Fossae region of Mars, *Science*, *302*, 627–630, doi:10.1126/science.1089647.

Holm, N. G., M. Dumont, M. Ivarsson, and C. Konn (2006), Alkaline fluid circulation in ultramafic rocks and formation of nucleotide constituents: A hypothesis, *Geochem. Trans.*, *7*, 7, doi:10.1186/1467-4866-7-7.

Huber, J. A., D. A. Butterfield, and J. A. Barros (2002), Temporal changes in archaeal diversity and chemistry in a mid-ocean ridge subseafloor habitat, *Appl. Environ. Microbiol.*, *68*, 1585–1594, doi:10.1128/AEM.68.4.1585-1594.2002.

Huse, S. M., L. Dethlefsen, J. A. Huber, D. M. Welch, D. A. Relman, and M. L. Sogin (2008), Exploring microbial diversity and taxonomy using SSU rRNA hypervariable tag sequencing, *PLoS Genet.*, *4*, e1000255, doi:10.1371/journal.pgen.1000255.

Huse, S. M., D. M. Welch, H. G. Morrison, and M. L. Sogin (2010), Ironing out the wrinkles in the rare biosphere through improved OUT clustering, *Environ. Microbiol.*, *12*, 1889–1898, doi:10.1111/j.1462-2920.2010.02193.x.

Jedryseck, M. O., and M. Sachanbiski (1994), Stable isotope and trace element studies of vein ophicarbonates at Gogolow-Jordanow serpentinite massif (Poland): A contribution to the origin of phiaragonite and ophimagnesite, *Geochem. J.*, *28*, 341–350.

Kelemen, P., and J. Matter (2008), In situ carbonation of peridotite for CO_2 storage, *PNAS*, *105*(45), 17,295–17,300, doi:10.1073/pnas.0805794105.

Kelemen, P. B., J. Matter, E. E. Streit, J. F. Rudge, W. B. Curry, and J. Blusztajn (2011), Rates and mechanisms of mineral carbonation in peridotite: Natural processes and recipes for enhanced, in situ CO_2 capture and storage, *Ann. Rev. Earth Planet. Sci.*, *39*(1), 545–576, doi:10.1146/annurev-earth-092010-152509.

Kelley, S. D., et al. (2001), An off-axis hydrothermal vent field near the Mid-Atlantic Ridge at 30°N, *Nature*, *412*, 145–149, doi:10.1038/35084000.

Kelley, D. S., et al. (2005), A serpentinite-hosted ecosystem: The lost city hydrothermal field, *Science*, *307*, 1428–1434, doi:10.1126/science.1102556.

Lang, S. Q., G. L. Früh-Green, S. M. Bernasconi, M. D. Lilley, G. Proskurowski, S. Mehay, and D. A. Butterfield (2012), Microbial utilization of abiogenic carbon and hydrogen in a serpentinite-hosted system, *Geochim. Cosmochim. Acta*, *92*, 82–99, doi:10.1016/j.gca.2012.06.006.

Lis, G. P., L. I. Wassenaar, and M. J. Hendry (2008), High-precision laser spectroscopy D/H and $^{18}O/^{16}O$ measurements of microliter natural water samples, *Anal. Chem.*, *80*(1), 287–293, doi:10.1021/ac701716q.

Macdonald, A. H., and W. S. Fyfe (1985), Rate of serpentinization in seafloor environments, *Tectonophysics*, *116*, 123–135, doi:10.1016/0040-1951(85)90225-2.

Marques, J. M., P. M. Carreira, M. R. Carvalho, M. J. Jatias, F. E. Goff, M. J. Basto, R. C. Graca, L. Aires-Barros, and L. Rocha (2008), Origins of high pH mineral waters from ultramafic rocks, Central Portugal, *Appl. Geochem.*, *23*, 3278–3289, doi:10.1016/j.apgeochem.2008.06.029.

Martin, W., and M. J. Russell (2007), On the origin of biochemistry at an alkaline hydrothermal vent, *Philos. Trans. R. Soc. B*, *362*, 1887–1925, doi:10.1098/rstb.2006.1881.

Matter, J., H. N. Waber, S. Loew, and A. Matter (2006), Recharge areas and geochemical evolution of groundwater in an alluvial aquifer system in the Sultanate of Oman, *Hydrogeol. J.*, *14*, 203–224, doi:10.1007/s10040-004-0425-2.

Matter, J., T. Takahashi, and D. Goldberg (2007), Experimental evaluation of in situ CO_2-water-rock reactions during CO_2 injection in basaltic rocks: Implications for geological CO_2 sequestration, *Geochem. Geophys. Geosyst.*, *8*, Q02001, doi:10.1029/2006GC001427.

McGuire, K. J., D. R. DeWalle, and D. J. Gburek (2002), Evaluation of mean residence in subsurface waters using oxygen-18 fluctuations during drought conditions in the mid-Appalachians, *Hydrology*, *261*, 132–149, doi:10.1016/S0022-1694(02)00006-9.
Morrill, P. L., J. G. Kuenen, O. J. Johnson, S. Suzuki, A. Rietze, A. L. Sessions, M. L. Fogel, and K. H. Nealson (2013), Geochemistry and geobiology of a present-day serpentinization site in California: The Cedars, *Geochim. Cosmochim. Acta*, *109*, 222–240, doi:10.1016/j.gca.2013.01.043.
Mulligan, M., and S. M. Burke (2005), Fog interception for the enhancement of streamflow in tropical areas (90 m resolution hydrological model), London, UK. [Available at http://www.ambiotek.com/fiesta, data base accessed 30 Sep. 2013.]
Myers, J. S., and J. L. Crowley (2000), Vestiges of life in the oldest Greenland rocks?: A review of early Archean geology in the Godthabsfjord region, and reappraisal of field evidence for >3850 Ma life on Akilia, *Precambrian Res.*, *103*, 101–124.
National Climatic Data Center (2013), *Climate Data Online: Search Tool*, Natl. Oceanic and Atmos. Admin., Asheville, NC, USA. [Avaliable at http://www.ncdc.noaa.gov/cdo-web/search, accesed 25 Nov. 2013.]
Neal, C., and G. Stanger (1983), Hydrogen generation from mantle source rocks in Oman, *Earth Planet. Sci. Lett.*, *66*, 315–320, doi:10.1016/0012-821X(83)90144-9.
Nisbet, E. G., and N. H. Sleep (2001), The habitat and nature of early life, *Nature*, *409*, 1083–1091, doi:10.1038/35059210.
O'Neil, J. R., and I. Barnes (1971), C13 and O18 compositions in some fresh-water carbonates associated with ultramafic rocks and serpentinites: Western United States, *Geochim. Cosmochim. Acta*, *35*, 687–697.
Paige, D. (2005), Ancient Mars: Wet in many places, *Science*, *307*, 1575–1576, doi:10.1126/science.1110530.
Palandri, J. L., and M. H. Reed (2004), Geochemical models of metasomatism in ultramafic systems: Serpentinization, rodingitization, and sea floor carnonate chimmey precipitation, *Geochim. Cosmochim. Acta*, *68*(5), 1115–1133, doi:10.1016/j.gca.2003.08.006.
Paukert, A. N., M. Jürg, P. B. Kelemen, E. L. Shock, and J. R. Havig (2012), Reaction path modeling of enhanced in situ CO_2 mineralization for carbon sequestration in the peridotite of the Samail Ophiolite, Sultanate of Oman, *Chem. Geol.*, *330–331*, 86–100, doi:10.1016/j.chemgeo.2012.08.013.
Pirard, C., J. Hermann, and H. St. C. O'Neill (2013), Petrology and geochemistry of the crust-mantle boundary in a nascent arc, Massif du Sud Ophiolite, New Caledonia, SW Pacific, *Petrology*, *54*(9), 1759–1792, doi:10.1093/petrology/egt030.
Proskurowski, G., M. D. Lilley, J. S. Seewald, G. L. Frueh-Green, E. J. Olson, J. E. Lupton, S. P. Sylva, and D. S. Kelley (2008), Abiogenic hydrocarbon production at Lost City Hydrothermal Field, *Science*, *319*, 604–607, doi:10.1126/science.1151194.
Quesnel, B., P. Gautier, P. Boulvais, M. Cathelineau, P. Maurizot, D. Cluzel, M. Ulrich, S. Guillot, S. Lesimple, and C. Couteau (2013), Syn-tectonic, meteoric water-derived carbonation of the New Caledonia peridotite nappe, *Geology*, *41*(10), 1063–1066, doi:10.1130/G34531.1.
Russell, M. J., and I. Kanik (2010), Why does life start, what Does it do, where might it be, how might we find it?, *J. Cosmol.*, *5*, 1008–1039.
Russell, M. J., A. J. Hall, and D. Turner (1989), In vitro growth of iron sulphide chimneys: Possible culture chambers for origin-of-life experiments, *Terra Nova*, *1*, 238–241, doi:10.1111/j.1365-3121.1989.tb00364.x.
Russell, M. J., R. M. Daniel, A. J. Hall, and J. Sherringham (1994), A hydrothermally precipitated catalytic iron sulphide membrane as a first step toward life, *J. Mol. Evol.*, *39*, 231–243.
Saginor, I., E. Gazel, C. Condie, and M. J. Carr (2013), Evolution of geochemical variations along the Central American volcanic front, *Geochem. Geophys. Geosyst.*, *14*, 4504–4522, doi:10.1002/ggge.20259.
Sanghyun, K., and J. Sungwon (2014), Estimation of mean water transit time on a steep hillslope in South Korea using soil moisture measurements and deuterium excess, *Hydrol. Processes*, *28*, 1844–1857, doi:10.1002/hyp.9722.
Sánchez-Murillo, R., G. Esquivel-Hernández, K. Welsh, E. S. Brooks, J. Boll, R. Alfaro-Solís, and J. Valdés-González (2013), Spatial and temporal variation of stable isotopes in precipitation across Costa Rica: An analysis of historic GNIP records, *Mod. Hydrol.*, *3*, 226–240, doi:10.4236/ojmh.2013.34027.
Schrenk, M. O., D. S. Kelley, J. R. Delaney, and J. A. Baross (2003), Incidence and diversity of microorganisms within the walls of an active deep-sea sulfide chimney, *Appl. Environ. Microbiol.*, *69*, 3580–3592, doi:10.1128/AEM.69.6.3580-3592.2003.
Schrenk, M. O., D. S. Kelley, S. A. Bolton, and J. A. Baross (2004), Low archaeal diversity linked to subseafloor geochemical processes at the Lost City Hydrothermal Field, Mid-Atlantic Ridge, *Environ. Microbiol.*, *6*(10), 1086–1095, doi:10.1111/j.1462-2920.2004.00650.x.
Schrenk, M. O., W. J. Brazelton, and S. Q. Lang (2013), Serpentinization, carbon, and deep life, *Rev. Mineral. Geochem.*, *75*, 575–606, doi:10.2138/rmg.2013.75.18.
Schulte, M., D. Blake, T. Hoehler, and T. McCollom (2006), Serpentinization and its implications for life on the early Earth and Mars, *Astrobiology*, *6*, 364–376, doi:10.1130/focus102010.1.
Schwarzenbach, E. M., G. L. Früh-Green, S. M. Bernasconi, J. C. Alt, and A. Plas (2013a), Serpentinization and the incorporation of carbon: A study of two ancient peridotite-hosted hydrothermal systems, *Chem. Geol.*, *351*, 115–133, doi:10.1016/j.chemgeo.2013.05.016.
Schwarzenbach, E. M., S. Q. Lang, G. L. Früh-Green, M. D. Lilley, S. M. Bernasconi, and S. Méhay (2013b), Sources and cycling of carbon in continental, serpentinite-hosted alkaline springs in the Voltri Massif, Italy, *Lithos*, *177*, 226–244, doi:10.1016/j.lithos.2013.07.009.
Shervais, J. W., P. Kolesar, and K. Andreasen (2005), A field and chemical study of serpentinization—Stonyford, California: Chemical fluxes and mass balance, *Int. Geol. Rev.*, *47*, 1–23, doi:10.2747/0020-6814.47.1.1.
Sogin, M. L., H. G. Morrison, J. A. Huber, D. M. Welch, S. M. Huse, P. R. Neal, J. M. Arrieta, and G. J. Herndl (2006), Microbial diversity in the deep sea and the underexplored "rare biosphere", *Proc. Natl. Acad. Sci. U. S. A.*, *103*, 12,115–12,120, doi:10.1073/pnas.0605127103.
Soulsby, C., D. Tetzlaff, and M. Hrachowitz (2009), Tracers and transit times: Windows for viewing catchment scale storage?, *Hydrol. Processes*, *23*, 3503–3507, doi:10.1002/hyp.7501.
Stewart, M. K., U. Morgenstern, J. J. McDonnell, and L. Pfister (2012), The 'hidden streamflow' challenge in catchment hydrology: A call to action for stream water transit time analysis, *Hydrol. Processes*, *26*, 2061–2066, doi:10.1002/hyp.9262.
Suzuki, S., S. Ishnii, A. Wu, A. Cheung, A. Tenney, G. Wanger, J. G. Kuenen, and K. Nealson (2013), Microbial diversity in The Cedars, and ultrabasic, ultrareducing, and low salinity serpentinizing ecosystem, *Proc. Natl. Acad. Sci. U. S. A.*, *110*(38), 15,336–15,341.
Szponar, N., W. J. Brazelton, M. O. Schrenk, D. M. Bower, A. Steele, and P. L. Morrill (2012), Geochemistry of a continental site of serpentinization, the Tablelands Ophiolite, Gros Morne National Park: A Mars analogue, *Icarus*, *224*, 286–296, doi:10.1016/j.icarus.2012.07.004.
Tournon, J., M. Seyler, and A. Astorga (1995), Les peridotites du Rio San Juan (Nicaragua et Costa Rica); jalons possibles d'une suture ultrabasique E-W en Amerique Centrale meridionale, *C. R. Acad. Sci., Ser. II*, *320*(8), 757–764.
Waylen, P., C. N. Caviedes, and M. E. Quesada (1996), Interannual variability of monthly precipitation in Costa Rica, *Climate*, *9*, 2506–2613.